Review Article | Neuroimaging and Head & Neck

eISSN 2005-8330
https://doi.org/10.3348/kjr.2020.1450
Korean J Radiol 2021

Korean Journal of Radiology
KJR

Pre- and Post-Treatment Imaging of Primary Central Nervous System Tumors in the Molecular and Genetic Era

Sung Soo Ahn[1, 2], Soonmee Cha[2]

[1]Department of Radiology, Severance Hospital, Research Institute of Radiological Science and Center for Clinical Image Data Science, Yonsei University College of Medicine, Seoul, Korea; [2]Department of Radiology and Biomedical Imaging, University of California San Francisco, San Francisco, CA, USA

Recent advances in the molecular and genetic characterization of central nervous system (CNS) tumors have ushered in a new era of tumor classification, diagnosis, and prognostic assessment. In this emerging and rapidly evolving molecular genetic era, imaging plays a critical role in the preoperative diagnosis and surgical planning, molecular marker prediction, targeted treatment planning, and post-therapy assessment of CNS tumors. This review provides an overview of the current imaging methods relevant to the molecular genetic classification of CNS tumors. Specifically, we focused on 1) the correlates between imaging features and specific molecular genetic markers and 2) the post-therapy imaging used for therapeutic assessment.

Keywords: *CNS tumor; Molecular marker; Magnetic resonance imaging; Positron emission tomography*

INTRODUCTION

Over the last decade, there has been an explosion of discoveries and advances in molecular and genetic profiling of central nervous system (CNS) tumors, ushering in a new era of brain tumor diagnostics and classification. The World Health Organization (WHO) 2016 classification of CNS tumors put forth an integrated diagnostic approach combining phenotypic and genotypic classifications that were based on key molecular markers [1]. This approach provided a general framework and concept for how CNS tumors should be diagnosed to improve prognostic stratification and treatment response predictions. With the current focus on precision medicine, the molecular and genetic characteristics of CNS tumors must be understood to gain insight into the biological behaviors and therapeutic responses of these tumors.

MRI is an integral part of CNS tumor evaluation for preoperative diagnosis, surgical and therapy planning, assessment of therapy response, and detection of recurrence. In addition to these critical roles in clinical practice, radiologic features may reflect histological and biological behaviors of the tumors and therefore may play an important role in the non-invasive prediction of molecular markers [2,3]. In addition, positron emission tomography (PET) has been used for brain tumor imaging with a variety of radioactive agents such as ^{11}C-methyl-L-methionine (MET), [^{18}F] fluoroethyl-L-tyrosine (FET), and 3,4-dihydroxy-6-[^{18}F]-fluoro-L-phenylalanine (FDOPA) [4,5]. Furthermore, treatment-related changes to tumor or normal brain tissues can frequently mimic tumor progression, making the use of imaging for assessing treatment response, including novel targeted and experimental therapies, more challenging [6,7].

This review aims to provide an overview of the correlates between imaging features and specific molecular genetic markers. Additionally, in this review, the advances

Received: December 11, 2020 **Revised:** April 8, 2021
Accepted: April 9, 2021
This research received funding from the Basic Science Research Program through the National Research Foundation of Korea (NRF) funded by the Ministry of Science, Information and Communication Technologies & Future Planning (2020R1A2C1003886).
Corresponding author: Soonmee Cha, MD, Department of Radiology and Biomedical Imaging, University of California San Francisco, 505 Parnassus Ave, San Francisco, CA 94143, USA.
• E-mail: Soonmee.Cha@ucsf.edu

in targeted therapy and the evolving role of imaging in response assessment following novel targeted and experimental therapies will be discussed.

Imaging Features and Molecular-Genetic Markers of CNS Tumors (Table 1)

Diffuse Gliomas

According to the 2016 WHO classification of CNS tumors, diffuse gliomas are graded from II to IV based on histological features and further classified based on the presence or absence of isocitrate dehydrogenase (IDH) mutations and 1p/19q codeletions (WHO grade II and III oligodendrogliomas, grade II and grade III astrocytic tumors, and grade IV glioblastomas) [1]. The remaining tumors that do not fit into the defined tumor types in the WHO 2016 classification are designated as not otherwise specified (NOS). In addition, the Consortium to Inform Molecular and Practical Approaches to CNS Tumor Taxonomy (cIMPACT-NOW) was formed and has published several guidelines (cIMPACT-NOW updates 1–7) to improve the diagnosis and classification of CNS tumors [8].

According to the 2016 WHO update, WHO grade II and III gliomas are largely categorized into astrocytomas or oligodendrogliomas based on molecular markers. WHO grade II and III oligodendroglial tumors, molecularly defined as IDH-mutant and 1p/19q codeleted tumors, tend to be located in the frontal lobe and present some degree of enhancement with ill-defined margins and calcifications. A previous study showed that, among IDH-mutant lower-grade gliomas, a less homogeneous texture, T2* blooming, a frontal location, and absent hydrocephalus were imaging features associated with 1p/19q codeletion [9]. Furthermore, advanced imaging parameters such as apparent diffusion coefficient (ADC), fractional anisotropy (FA, MAPK, iRANO, LITT), and cerebral blood volume (CBV) have been reported as potentially useful parameters for prediction of 1p/19q codeletion status [3,10]. WHO grade II diffuse astrocytomas and grade III anaplastic astrocytomas are each further divided into IDH-mutant and IDH-wildtype. Infiltrating gliomas that harbor IDH mutations but not 1p/19q codeletions are classified as diffuse astrocytoma, IDH-mutant, and the T2-fluid-attenuated inversion-recovery (FLAIR) mismatch sign, in which tumors that are homogenously hyperintense on T2WI and internally hypointense on FLAIR, was reported as an imaging biomarker highly specific for this molecular subtype (Fig. 1) [11]. Lower-grade gliomas (WHO grade II and III) with IDH wildtype have demonstrated molecular alterations and biological behaviors similar to those of primary glioblastoma [12]. Therefore, the reliable non-invasive identification of IDH mutations may be useful for treatment planning, and a variety of morphologic and MRI features have been correlated with IDH mutation status in diffuse gliomas. Although lower-grade gliomas generally appear as T2 hyperintense expansile masses involving both the cortex and underlying white matter with variable enhancement, IDH-wildtype gliomas are more likely to have a multifocal, non-lobar location and show more contrast enhancement, poor margin definition, low ADC, and high relative CBV (Fig. 2) in accordance with the genomic analysis results [3,13,14]. Several studies using traditional machine learning and deep learning to predict IDH mutation status in diffuse gliomas using preoperative MRIs have also had promising results [15,16]. In addition, IDH mutations can be directly detected through increased levels of D-2-hydroxyglutarate, which can be quantified using MR spectroscopy with a high sensitivity and specificity [17]. Previous studies have also shown that FET-PET is associated with IDH mutation status, although the biochemical relationship is not well-understood [18,19].

Even though IDH-wildtype astrocytoma has a worse prognosis than IDH-mutant astrocytoma, patients with IDH-wildtype astrocytomas have been shown to have variable survival outcomes. Therefore, cIMPACT-NOW recommends that IDH-wildtype astrocytoma with one of the three genetic markers (epidermal growth factor receptor [EGFR] amplification, telomerase reverse transcriptase [TERT] promoter mutation, and the combined whole chromosome 7 gain and 10 loss) should be diagnosed as glioblastoma [8]. A recent study demonstrated that IDH-wildtype astrocytomas with EGFR amplification had lower ADC, and those with TERT mutations had higher plasma volume fractions [20].

Glioblastoma is the most common primary parenchymal brain tumor and the most common glioma, with a median survival of 15–18 months and a high rate of recurrence following initial standard treatment [21]. Glioblastoma is a heterogeneous tumor that is characterized by irregular margins, heterogeneous enhancement with varying degrees of necrosis, edema, and intratumoral hemorrhage. According to the 2016 WHO classification of CNS tumors, the molecular subtypes of glioblastomas are divided into two types: IDH-wildtype and IDH-mutant. IDH-mutant

https://doi.org/10.3348/kjr.2020.1450

Korean Journal of Radiology
KJR

Table 1. Imaging Features and Molecular-Genetic Markers of CNS Tumors

Pathology	WHO Grade	Molecular-Genetic Markers	Common Imaging Features
Oligodendroglioma	II/III	IDH-mutant and 1p/19q codeletion	Frontal lobe location Variable enhancement Ill-defined margin Calcifications T2* blooming Heterogeneous texture Mixed diffusion restriction
Diffuse astrocytoma	II/III	IDH mutant, 1p/19q non-codeletion	T2-FLAIR mismatch sign
		IDH wildtype	Multifocal Non-lobar location More contrast enhancement Poor margin Low ADC High relative CBV High APT
Glioblastoma	IV	IDH wildtype	Intratumoral necrosis More contrast enhancement Low ADC High relative CBV
		MGMT promoter methylation	Loss edema High ADC Low relative CBV
Pilocytic astrocytoma	I	BRAF and KIAA1549 (> 70%)	Well-circumscribed cystic mass with mural nodule Little peritumoral edema High ADC
Pleomorphic xanthoastrocytoma	II/III	$BRAF^{V600E}$ mutation (> 60%)	Cystic mass with enhancing mural nodule
Rosette-forming glioneuronal tumor	I	Synaptophysin	Fourth ventricle and aqueduct of Sylvius Circumscribed tumor with variable solid-cystic components
Diffuse leptomeningeal glioneuronal tumor	Not assigned	OLIG2, S-100	Diffuse leptomeningeal enhancement, with or without a parenchymal component
Ependymoma	II/III	RELA fusion	Supratentorial location Heterogeneous large mass with solid and cystic components Intratumoral hemorrhage Peritumoral edema Low ADC
Medulloblastoma	IV	WNT-activated	Cerebellar peduncle, cerebellopontine angle cistern
		SHH-activated	Cerebellar hemispheres
		Group 3	Cerebellar vermis and fourth ventricle Early metastasis
		Group 4	Cerebellar vermis and fourth ventricle Minimal or no enhancement
ETMR	IV	C19MC-altered	Large Frequent calcifications Little edema Absent or weak enhancement Intratumoral veins Low ADC Low CBF

https://doi.org/10.3348/kjr.2020.1450

Table 1. Imaging Features and Molecular-Genetic Markers of CNS Tumors (Continued)

Pathology	WHO Grade	Molecular-Genetic Markers	Common Imaging Features
Atypical teratoid/ rhabdoid tumor	IV	Loss of INI1 expression	Heterogeneous signal intensity Low ADC
Solitary fibrous tumor/ hemangiopericytoma	I/II/III	STAT6 nuclear expression	Vivid enhancement Dural tail Erosion of adjacent bone

ADC = apparent diffusion coefficient, APT = amide proton transfer, CBF = cerebral blood flow, CBV = cerebral blood volume, CNS = central nervous system, ETMR = embryonal tumor with multilayered rosettes, FLAIR = fluid-attenuated inversion-recovery, IDH = isocitrate dehydrogenase, MGMT = O6-methylguanine methyltransferase, SHH = Sonic Hedgehog, WNT = wingless

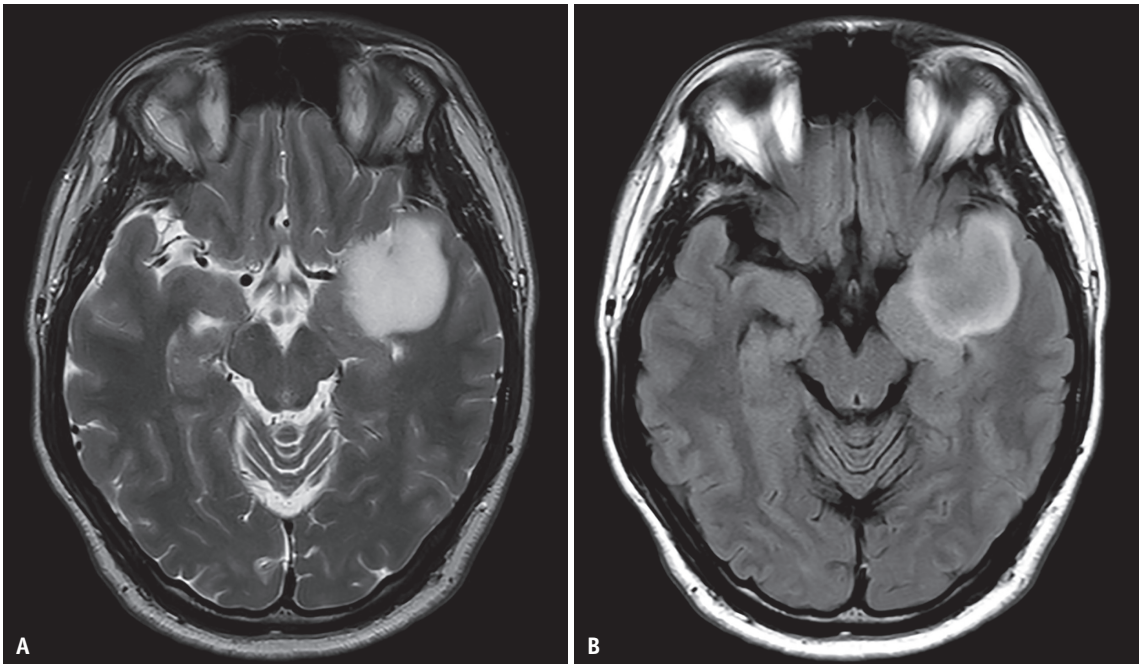

Fig. 1. A 32-year-old male with diffuse astrocytoma, isocitrate dehydrogenase-mutant, showing T2-FLAIR mismatch sign.
A. T2-weighted image. **B.** FLAIR image. FLAIR = fluid-attenuated inversion-recovery

glioblastomas correspond to what were previously called secondary glioblastomas, which were tumors that started as a lower-grade diffuse astrocytoma before undergoing malignant transformation. IDH-mutant glioblastomas have been reported to have less aggressive imaging features and less intratumoral necrosis, less contrast enhancement, higher ADC values, and less hyperperfusion than IDH-wildtype glioblastoma (Fig. 3) [13,22,23]. O6-methylguanine methyltransferase (MGMT) promoter methylation is considered a predictive biomarker for alkylating chemotherapy in glioblastoma [24]. Several studies have reported the use of imaging features for the prediction of MGMT promoter methylation, which include less edema, high ADC, and low perfusion, which are present in MGMT promoter methylated glioblastoma [25].

Diffuse midline glioma, H3 K27M-mutant, which is classified as WHO grade IV, is a new entity in the 2016 WHO classification of CNS tumors that is defined as an infiltrative glioma involving midline structures such as the thalamus, brain stem, spinal cord, and an H3 K27M mutation. H3 K27M mutation occurs predominantly in children and the expansile tumors involving pons with variable infiltration into the midbrain, medulla, and cerebellum were previously referred to as diffuse intrinsic pontine glioma. However, one-third of midline gliomas do not harbor the H3 K27M mutation [26]. A recent study reported that there were no imaging features that were significantly associated with the H3 K27M mutation for midline gliomas [27]. Another study of spinal cord gliomas also demonstrated heterogeneous imaging features of diffuse midline gliomas, and hemorrhage was the only distinct feature of H3 K27M-mutated diffuse midline glioma [28].

https://doi.org/10.3348/kjr.2020.1450

Korean Journal of Radiology
KJR

Circumscribed Gliomas

Pilocytic astrocytoma (WHO grade I) typically occurs in children and young adults. Common locations are the cerebellum, optic nerve, cerebrum, and brainstem. Although pilocytic astrocytoma is typically a well-circumscribed cystic mass with intramural nodules and minimal peritumoral

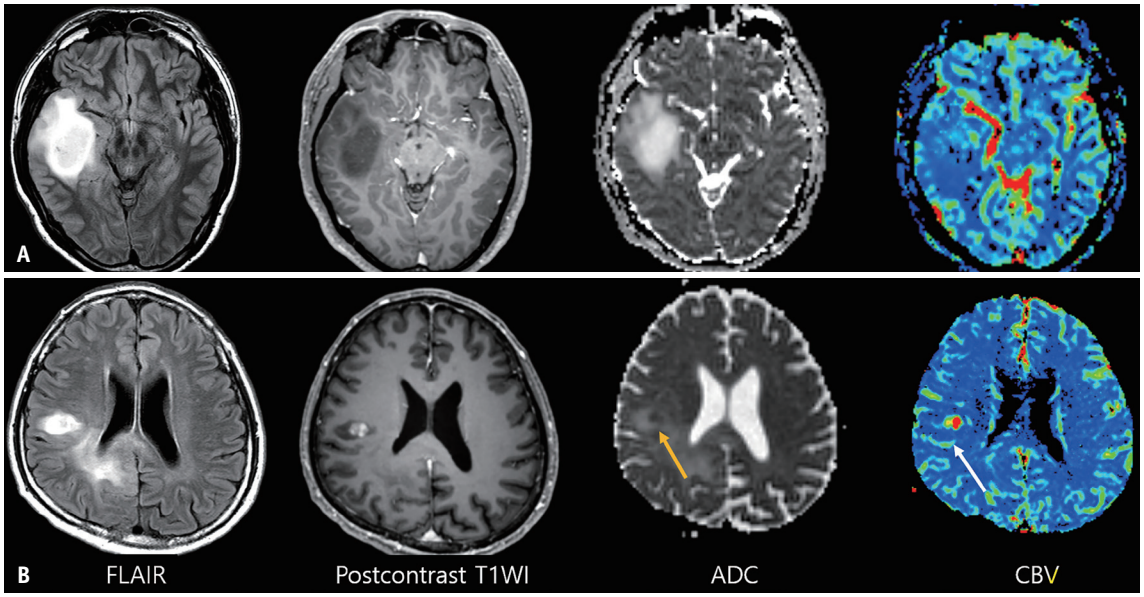

Fig. 2. Anaplastic astrocytomas, IDH-mutant and IDH-wildtype.
A. Anaplastic astrocytoma, IDH-mutant. MRI shows well-defined T2 hyperintense mass in the right temporal lobe on FLAIR with no definite enhancement on postcontrast T1WI. ADC map shows facilitated diffusion and CBV is not increased within the mass. **B.** Anaplastic astrocytoma, IDH-wildtype. An ill-defined infiltrative mass is seen in the right parietal lobe crossing the corpus callosum on FLAIR with focal enhancement on postcontrast T1WI. Diffusion restriction, showing low ADC, and high CBV are noted within the solid enhancing portion (arrows). ADC = apparent diffusion coefficient, CBV = cerebral blood volume, FLAIR = fluid-attenuated inversion-recovery, IDH = isocitrate dehydrogenase, T1WI = T1-weighted image

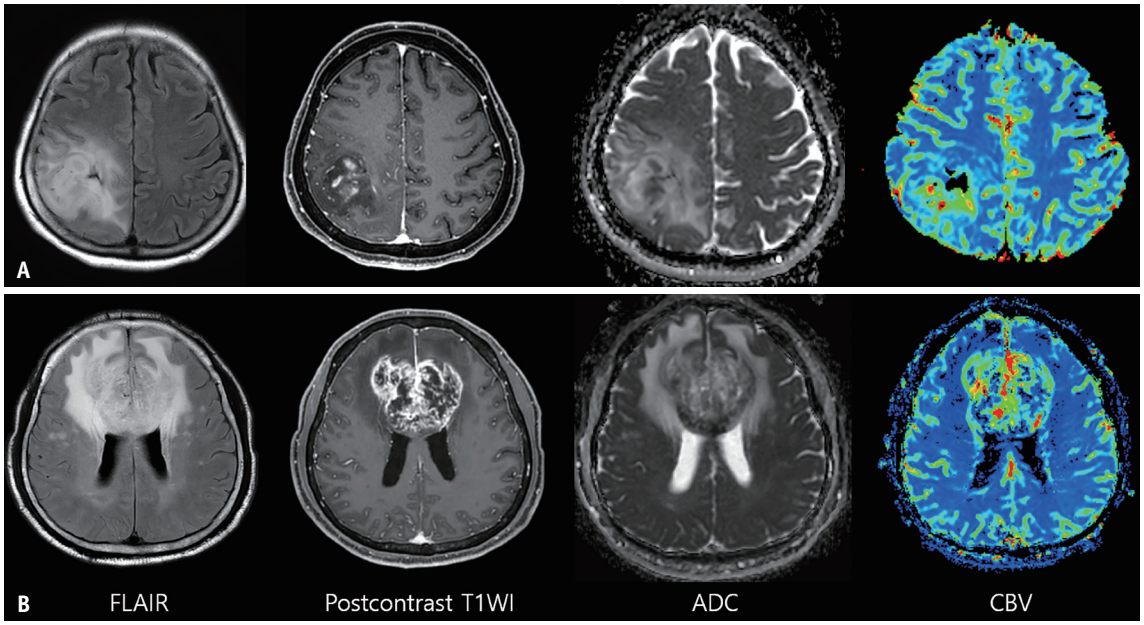

Fig. 3. Glioblastomas, IDH-mutant and IDH-wildtype.
A. Glioblastoma, IDH-mutant. MRI shows infiltrative mass in the right parietal lobe on FLAIR with multifocal enhancement on postcontrast T1WI. Diffusion restriction, showing low ADC, and high CBV are noted within the solid enhancing portion. **B.** Glioblastoma, IDH-wildtype. Heterogeneously enhancing mass with intratumoral necrosis and peritumoral edema involving the corpus callosum and bilateral frontal lobes. The mass shows diffusion restriction and a marked increase in the CBV. ADC = apparent diffusion coefficient, CBV = cerebral blood volume, FLAIR = fluid-attenuated inversion-recovery, IDH = isocitrate dehydrogenase, T1WI = T1-weighted image

https://doi.org/10.3348/kjr.2020.1450

edema, it may present as a mass with heterogeneous enhancement mimicking high-grade tumors. In these cases, the most useful indications for correct diagnosis are the imaging features related to low cellularity showing hyperintensity on T2WI and increased diffusion on diffusion-weighted image (DWI) [29].

Pilomyxoid astrocytoma, an uncommon variant of pilocytic astrocytoma, is commonly located in the hypothalamic/chiasmatic region. Although there is extensive histological and genetic overlap with pilocytic astrocytoma, pilomyxoid astrocytomas are predominantly solid and rarely have cystic components, in contrast to typical pilocytic astrocytomas [30].

Pleomorphic xanthoastrocytoma (PXA) exhibits a $BRAF^{V600E}$ mutation. BRAF is an oncogene located on chromosome 7q34 and a crucial regulator of the mitogen-activated protein kinase (MAPK) signaling pathway [31]. The $BRAF^{V600E}$ mutation is detected at a high frequency in PXA, ganglioglioma, and extra-cerebellar pilocytic astrocytoma [32], and these tumors typically demonstrate cystic masses with enhancing mural nodules (Fig. 4). In addition, PXA may exhibit a dural tail from reactive change and skull remodeling.

Glioneuronal Tumors

Ganglioglioma (WHO grade I), also commonly harboring the $BRAF^{V600E}$ mutation, is a slow-growing tumor composed of dysplastic ganglion cells and neoplastic glial cells and can occur anywhere throughout the craniospinal axis with a predilection for the temporal lobe [33]. Rosette-forming glioneuronal tumors (WHO grade I) are rare and predominantly involve the fourth ventricle and aqueduct of Sylvius and may have variable solid-cystic components [34]. Diffuse leptomeningeal glioneuronal tumors that express synaptophysin in addition to OLIG2 and S-100 are newly recognized in the 2016 WHO classification and present as diffuse leptomeningeal disease with or without a parenchymal component (Fig. 5) [1].

Ependymomas

Ependymomas are glial brain tumors that can arise from any of the CNS compartments, and recent extensive molecular analyses have revealed that supratentorial and posterior fossa ependymomas have distinct molecular profiles and are genetically different diseases [35]. Ependymoma, RELA fusion-positive was recognized in the 2016 WHO classification of CNS tumors as a distinct clinicopathological entity accounting for 70% of supratentorial tumors in children and has the worst prognosis among the supratentorial ependymomas [1,36]. Supratentorial ependymomas often present as large masses that appear heterogeneous, with both solid and cystic components (Fig. 6). A recent study reported that RELA fusion-positive ependymomas are frequently associated with intratumoral hemorrhage, peritumoral edema, diffusion restriction, prominent cysts, and necrosis [37].

Embryonal Tumors

Embryonal tumors are poorly differentiated tumors of neuroepithelial origin and, as a group, underwent substantial changes in the 2016 WHO classification. Specifically, genetically defined subtypes of

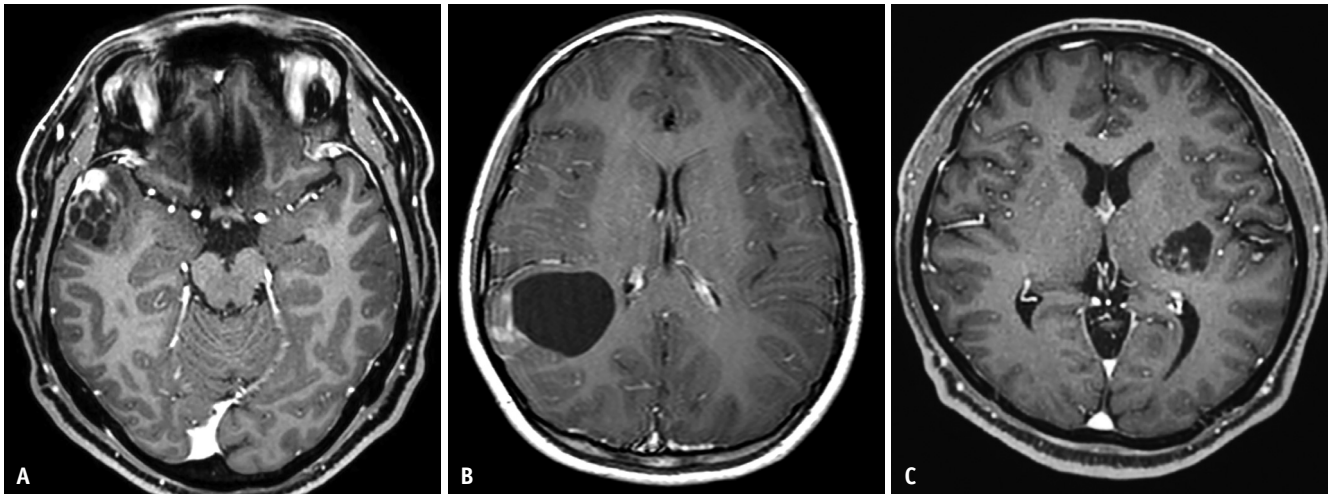

Fig. 4. Common imaging features of gliomas harboring the $BRAF^{V600E}$ mutation: a cystic mass with enhancing mural nodule; pleomorphic xanthoastrocytoma (A), ganglioglioma (B), pilocytic astrocytoma (C).

https://doi.org/10.3348/kjr.2020.1450

Korean Journal of Radiology
KJR

medulloblastomas were added, the CNS primitive neuroectodermal tumor classification was removed, and embryonal tumor with multilayered rosettes (ETMR), C19MC-altered, defined by amplification or gain of the C19MC region on chromosome 19, was newly described [1].

The 2016 WHO classification defines medulloblastoma

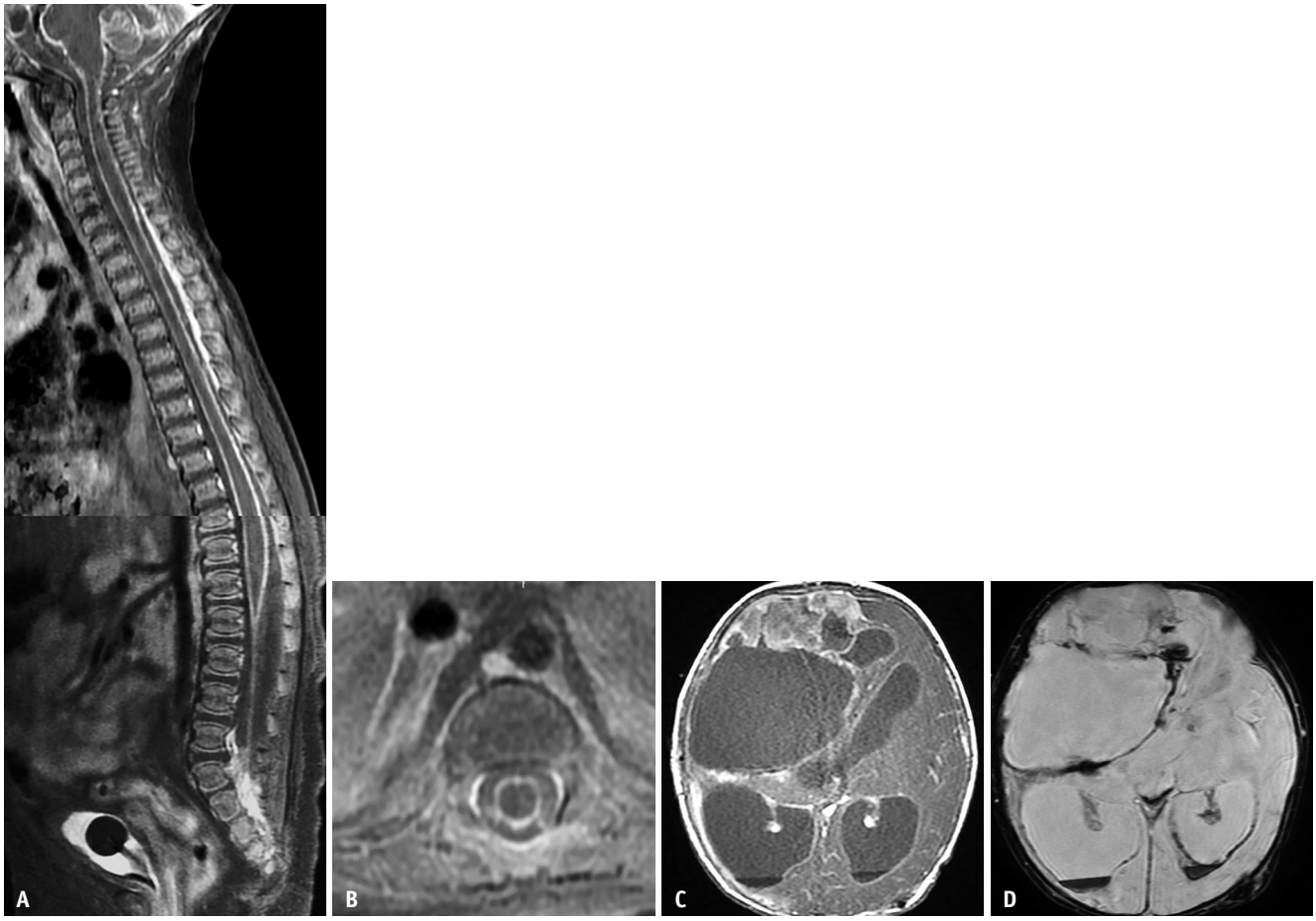

Fig. 5. An 11-week-old girl with a diffuse leptomeningeal glioneuronal tumor.
A-D. Sagittal **(A)** and axial **(B)** postcontrast T1WI show diffuse leptomeningeal enhancement along the spinal cord and brain stem. A large cystic mass with an enhancing solid portion is noted in the right frontal lobe on postcontrast T1WI **(C)**. Diffuse enhancement along the ependymal lining with hydrocephalus is also noted. Gradient echo imaging **(D)** demonstrates intratumoral hemorrhage combined with intraventricular hemorrhage. T1WI = T1-weighted image

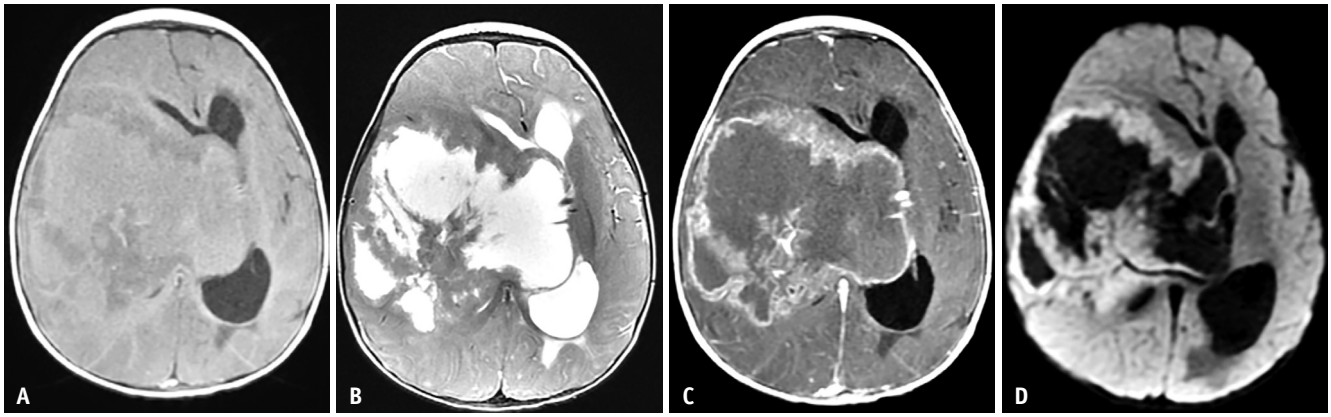

Fig. 6. A 7-month-old boy with ependymoma, RELA fusion-positive.
A-D. Huge mass with necrosis is seen in the right cerebral hemisphere on precontrast T1WI **(A)**, T2-weighted image **(B)**, postcontrast T1WI **(C)**, and diffusion-weighted image **(D)**. T1WI = T1-weighted image

https://doi.org/10.3348/kjr.2020.1450

both histologically and genetically. Histologically, four variants of medulloblastoma have long been established: classic, desmoplastic/nodular, extensive nodularity, and anaplastic/large cell. More recently, four distinct molecular subgroups have been identified based on genomic profiles: wingless (WNT)-activated, Sonic Hedgehog (SHH)-activated and TP53-mutant, SHH-activated and TP53-wildtype, and non-WNT/non-SHH consisting of Group 3, and Group 4. Molecular subgroups have been shown to correlate with clinical outcomes [38], and it has been suggested that MRI features can be helpful to predict the molecular subgroups preoperatively (Fig. 7) [39,40]. Specifically, WNT arises from the lower rhombic lip and therefore predominantly occurs in the cerebellar peduncle/cerebellopontine angle cistern, SHH occurs in the cerebellar hemispheres, and Groups 3 and 4 occur in the midline involving the cerebellar vermis and fourth ventricle [39,41]. In addition, minimal or no enhancement is a diagnostic indicator of Group 4, and a small midline tumor association with early metastasis suggests Group 3 [42].

ETMR, C19MC-altered refers to tumors formerly known as embryonal tumors with abundant neuropil and true rosettes and ependymoblastoma [1]. Any childhood CNS tumor with alterations at chromosome 19 (C19MC amplification) is now classified as ETMR, regardless of histology. ETMR mostly occurs in children under 2 years of age and is more often supratentorial. Although there is significant overlap in the radiologic appearance of embryonal tumors, the characteristic imaging features of ETMR, C19MC-altered include large tumor size with frequent calcifications, little-to-no edema, absent or weak contrast enhancement, intratumoral veins, restricted diffusion, and low cerebral blood flow values using arterial-spin-labeling MRI have been reported (Fig. 8) [43].

Atypical teratoid/rhabdoid tumor (AT/RT), genetically defined by a loss of INI1 expression, is aggressive and tends to affect infants. AT/RT should be considered when encountering striking heterogeneous tumors of the CNS with high cellularity on MRI in the pediatric population, especially in those aged < 4 years [44].

Solitary Fibrous Tumor/Hemangiopericytoma

In the 2016 WHO classification, the combined term solitary fibrous tumor/hemangiopericytoma was used to describe mesenchymal non-meningothelial tumors with STAT6 nuclear expression, which includes previously referred solitary fibrous tumor (grade I), hemangiopericytoma (grade II), and anaplastic hemangiopericytoma (grade III)

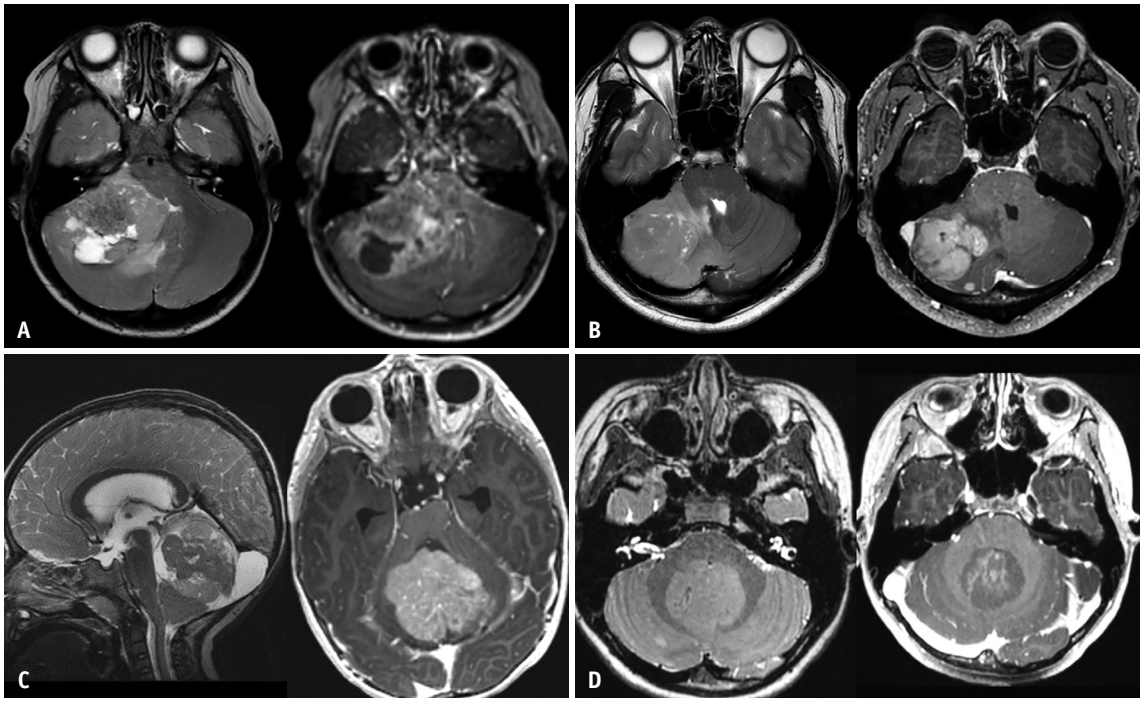

Fig. 7. Characteristic MRI features according to medulloblastoma molecular subgroups.
A. Wingless subgroup predominantly occurs in the cerebellar peduncle/cerebellopontine angle cistern. **B.** Sonic Hedgehog subgroup is predominantly located in the cerebellar hemispheres. **C, D.** Group 3 **(C)** and Group 4 **(D)** tumors are commonly located in the midline involving the cerebellar vermis and the fourth ventricle. Group 4 tumor tends to show minimal-to-no enhancement.

https://doi.org/10.3348/kjr.2020.1450

Korean Journal of Radiology
KJR

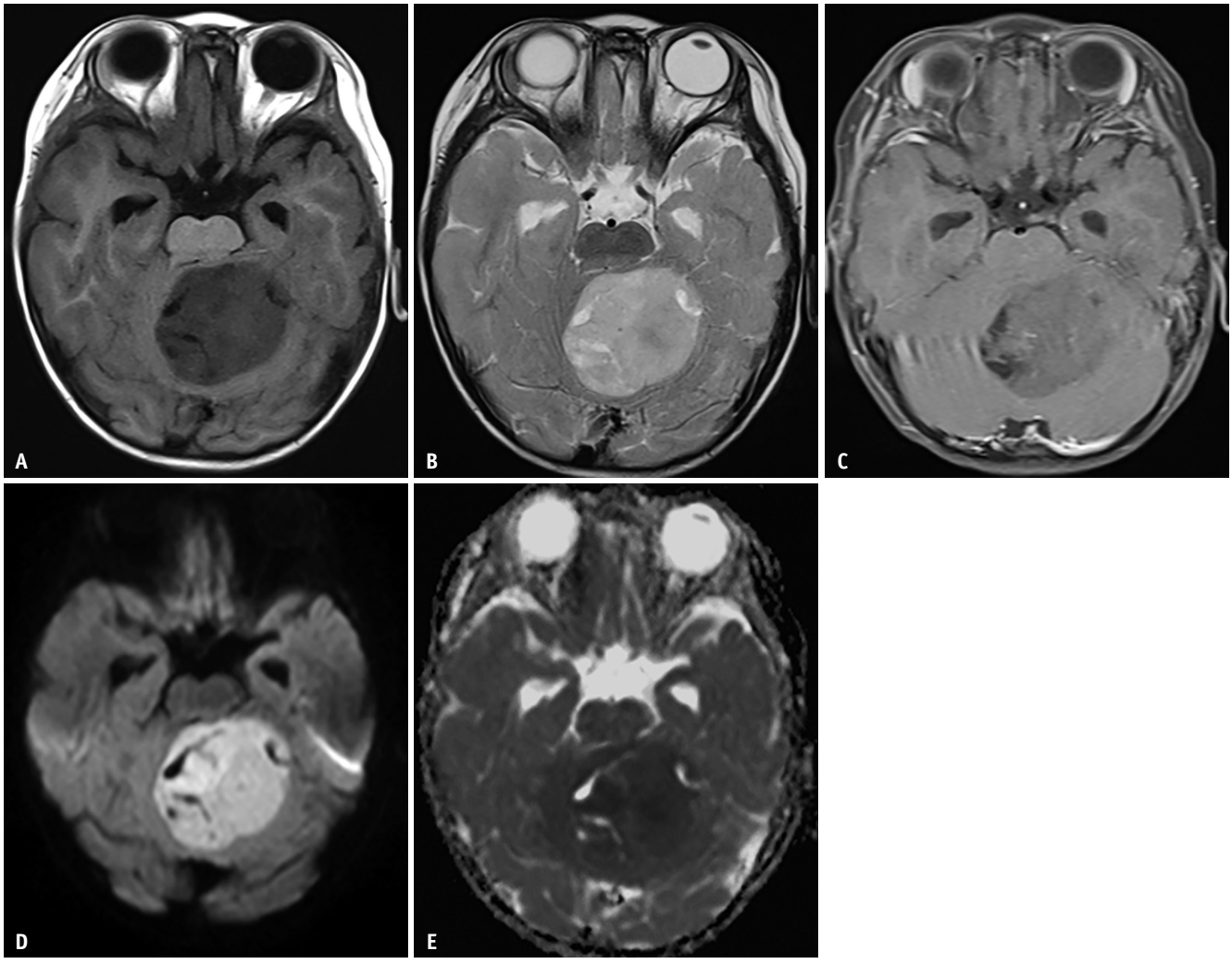

Fig. 8. A 2-year-old girl with embryonal tumor with multilayered rosettes, C19MC-altered.
A-E. The mass shows low signal intensity on T1WI **(A)** and high signal intensity on T2-weighted image **(B)**. There is no peritumoral edema or enhancement on postcontrast T1WI **(C)**. Diffusion is restricted within the mass on diffusion-weighted image **(D)** and the apparent diffusion coefficient map **(E)**. T1WI = T1-weighted image

[1]. Solitary fibrous tumor/hemangiopericytoma exhibits radiographic features similar to those of meningioma, with vivid enhancement and the dural tail sign, but tends to erode adjacent bone [45].

Post-Therapy Imaging of CNS Tumors (Table 2)

MRIs play an important role in monitoring tumor burden over the course of treatment; however, the accurate assessment of disease status is challenging due to the complex combination of therapies and treatment-related changes. As novel treatment approaches rapidly evolve and tumor appearance can be modified through therapy, it is important for radiologists to be aware of the imaging findings related to each treatment to accurately assess treatment response.

A postoperative baseline MRI should ideally be obtained within 24 to 48 hours of surgery (especially for high-grade glioma) to avoid misinterpreting postoperative changes as residual enhancing tumor since postoperative enhancement can be seen along the resection margins by 48–72 hours post-operation. In addition, diffusion restriction around the resection cavity, which is related to direct trauma and vascular injury, can occur following surgery, potentially mimicking recurrent tumors on follow-up imaging [46]. Therefore, enhancement on follow-up imaging after surgery should be carefully interpreted with reference to the DWI obtained in the immediate postoperative period.

Pseudoprogression, defined as a new or enlarging contrast-enhancing lesion followed by subsequent improvement

 https://doi.org/10.3348/kjr.2020.1450

without any change in treatment, occurs in 20–30% of patients with glioblastoma within 3 months of concurrent chemoradiotherapy (CCRT) [47]. Cytotoxic therapies not only damage tumor vessels and normal brain tissue but can also induce inflammatory responses in microglia, which can induce a pronounced blood-brain barrier disruption and a transient increase in enhancement on MRI. Therefore, the Response Assessment for the Neuro-Oncology (RANO) working group has recommended that within 3 months of CCRT, progression be confirmed only if the majority of the new enhancement is outside of the radiation field or if there is pathologic confirmation of disease progression [47]. To identify early tumor progression, the development of imaging biomarkers would be ideal. However, conventional MRIs do not allow for a reliable distinction between treatment-related changes and true progression, as both may share imaging features of mass effect, perilesional edema, and contrast agent enhancement due to blood-brain barrier breakdown. In addition, variable treatment-related effects and recurrent tumors are frequently combined. Although surgical sampling or follow-up imaging may be necessary for a definitive diagnosis, imaging modalities such as perfusion imaging, MR spectroscopy, and PET scans have been extensively investigated and may sometimes be helpful for differentiating treatment effects from recurrent tumors [4,6].

Previous studies have shown that relative CBV from Dynamic susceptibility contrast imaging and K^{trans} and Ve from DCE imaging may be helpful for differentiating between true progression and pseudoprogression [7,48,49]. In addition, perfusion MRIs significantly improved the prediction of recurrent glioblastoma in combination with postcontrast T1-weighted image and DWI [6]. Another study showed that multiparametric radiomics can be helpful for identifying pseudoprogression with good generalizability [50]. In another study, amide proton transfer imaging has added value to other advanced imaging parameters for distinguishing between recurrent

Table 2. Post-Therapy Imaging Features

Therapy	Treatment-Related Changes	Common Imaging Features
Concurrent chemoradiotherapy	Pseudoprogression	New or enlarging contrast-enhancing lesion within 3 months after therapy and subsequent improvement on follow-up
Antiangiogenic therapy	Pseudoresponse	Decrease in contrast enhancement with progressive increase in nonenhancing T2 hyperintense lesion
Immunotherapy	Pseudoprogression	New or enlarging contrast-enhancing lesion within 6 months of initiating therapy followed by improvement on follow-up
Convection-enhanced delivery therapy	Gadolinium administered along with therapeutics	High signal intensity mimicking enhancing tumor
Laser interstitial thermal therapy	Reactive inflammation or granulation tissue	Thin peripheral rim enhancement within 24 hours, which tends to enlarge during the first 40 days followed by a continuous reduction

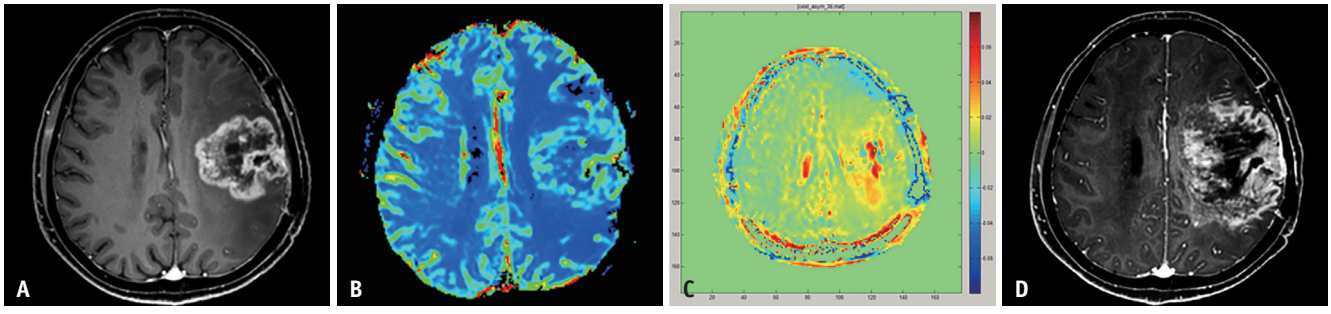

Fig. 9. A 65-year-old female presenting with an enhancing mass in the left frontoparietal lobe on MRI after postoperative concurrent chemoradiotherapy for glioblastoma (A). The mass demonstrates a mild increase in relative cerebral blood volume (B) and an increase in the amide proton transfer signal (C). The follow-up MRI shows increased enhancing mass (D), suggesting recurrent glioblastoma.

https://doi.org/10.3348/kjr.2020.1450

Korean Journal of Radiology
KJR

gliomas and treatment-induced changes (Fig. 9) [51]. A recent meta-analysis showed the highest diagnostic accuracy for MR spectroscopy, followed by perfusion imaging, and all advanced MRI techniques had higher diagnostic accuracy than conventional MRIs [52]. Amino acid PET using FET and FDOPA has been increasingly used as a tracer for brain tumor imaging and has been useful in differentiating tumor progression from treatment-induced changes with a diagnostic accuracy ranging 80–90% (Fig. 10) [5,53]. The diagnostic performance of MET PET seems to be slightly lower, with an accuracy of approximately 75% [54].

Antiangiogenic Therapy

Angiogenesis is the process by which tumors develop additional blood vessels from pre-existing vessels to provide oxygen and nutrients for tumor expansion, and tumor vasculature formed by neoangiogenesis is structurally and functionally abnormal. Antiangiogenic agents normalize tortuous and leaky tumor vasculature so that drug and

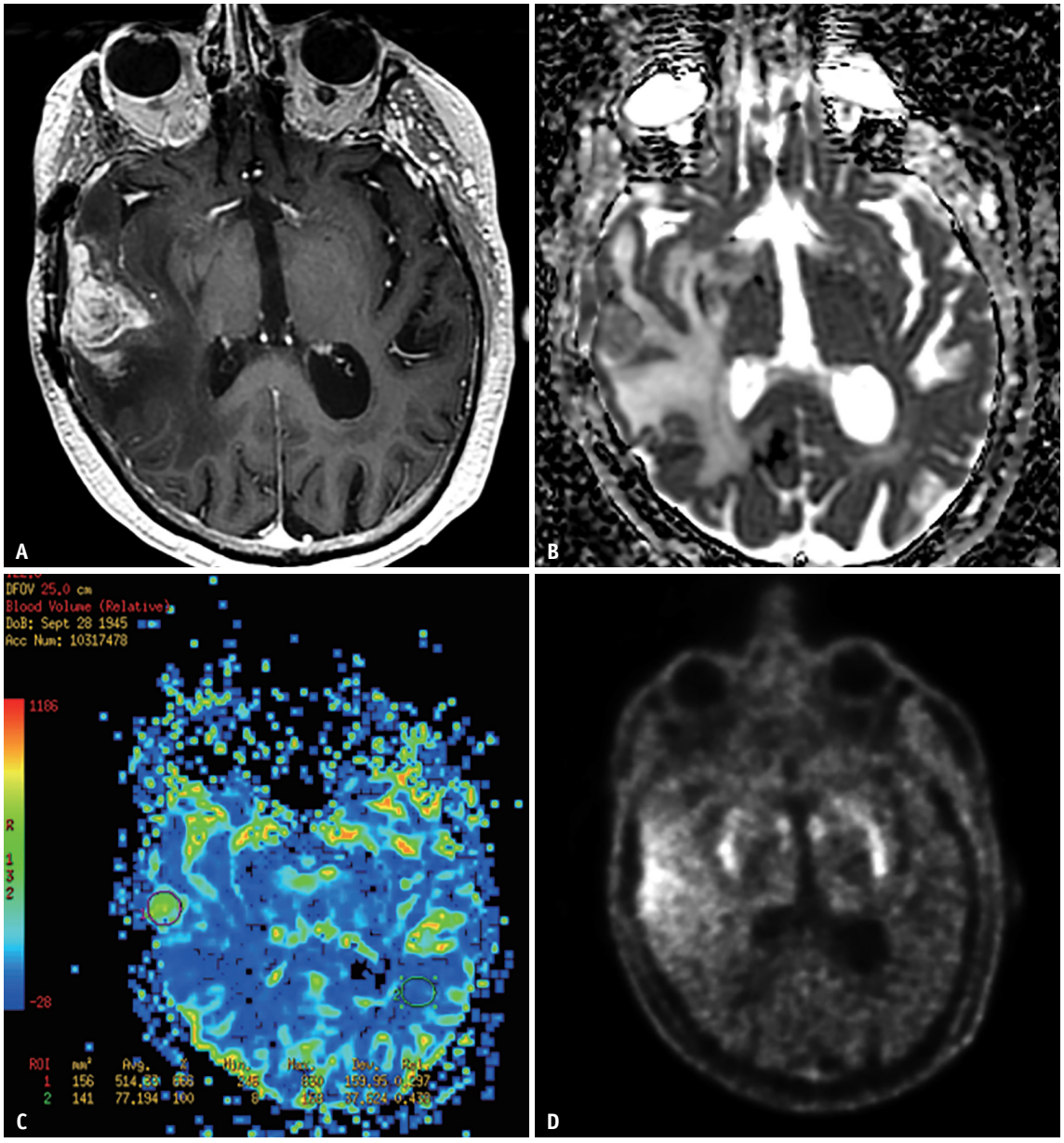

Fig. 10. Recurrent glioblastoma in the right temporal lobe shows heterogeneous enhancement with marked perilesional edema on postcontrast T1-weighted image (A). Diffusion is restricted on the apparent diffusion coefficient map (B) and cerebral blood volume is mildly increased (C). 3,4-dihydroxy-6-[^{18}F]-fluoro-L-phenylalanine-PET demonstrates increased uptake in the corresponding area (D).

https://doi.org/10.3348/kjr.2020.1450

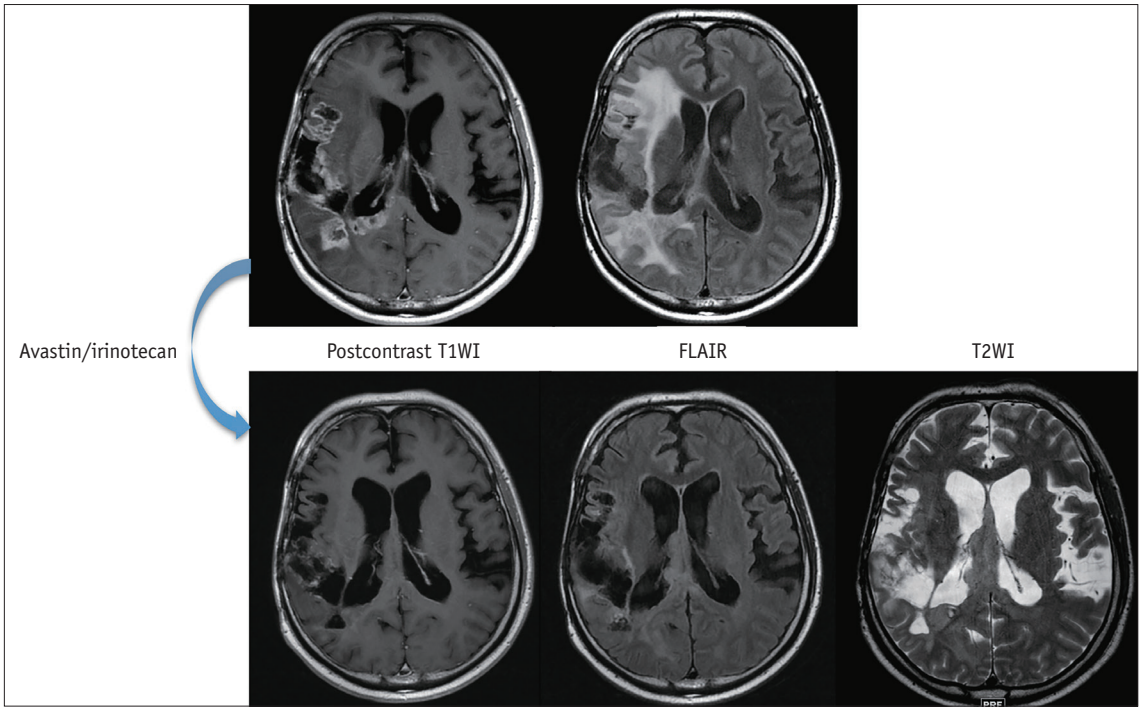

Fig. 11. Recurrent glioblastoma in a 37-year-old male with heterogeneous enhancement along the resection margin on postcontrast T1WI and marked perilesional edema (upper row). After 10 cycles of Avastin and Irinotecan, contrast enhancement and edema improved significantly. However, FLAIR and T2WI demonstrate nonenhancing nodular lesions along the septum pellucidum, which suggests pseudoresponse. FLAIR = fluid-attenuated inversion-recovery, T1WI = T1-weighted image, T2WI = T2-weighted image

oxygen delivery is more efficient, leading to a significant decrease in contrast enhancement in most patients, though this may not necessarily indicate an antitumor effect. Sometimes tumors become more infiltrative and show an aggressive phenotype after antiangiogenic therapy (Fig. 11). Therefore, a decrease in enhancement with a progressive increase in the non-enhancing portion is referred to as pseudoresponse and RANO incorporated non-enhancing T2 hyperintense lesions as well as enhancing lesions for response assessment to better evaluate the effect of antiangiogenic therapy [47]. Diffusion-restricted lesions may appear within the previously enhanced tumor area on follow-up imaging after antiangiogenic therapy, and conflicting results have been reported, with these regions either developing atypical necrosis or hypercellular tumors. A previous report showed that the pathology obtained in diffusion-restricted lesions revealed an infiltrative tumor with dense cellularity [55]. In contrast, another study found that pathology showed atypical necrosis and the accumulation of HIF-1a in diffusion-restricted lesions [55]. In a recent study of postmortem brain specimens, progressively expanding diffusion restriction was predominantly coagulative necrosis surrounded by a viable hypercellular tumor [56].

Immunotherapy

Immunotherapy has emerged as a promising therapeutical strategy, and a wide range of immunotherapies are currently being investigated for brain tumors, from immune-checkpoint blockage, vaccination therapy, oncolytic viral therapy, and chimeric antigen receptor (CAR) T cell therapy [57].

Immune checkpoint inhibitors are monoclonal antibodies to PD-1 (nivolumab, pembrolizumab), PD-L1, and cytotoxic T-lymphocyte antigen-4 (ipilimumab) that promote immune system-mediated tumor destruction by inhibiting the signaling pathways that suppress antitumor T cell activity.

Vaccine therapy aims to activate a successful immune response and effective T cell cytotoxicity in the tumor microenvironment. Using different tumor-associated antigens, such as EGFR variant III and IDH, peptide vaccines are directly administered to the patient to prime the immune system to recognize cells presenting that antigen [57]. Dendritic cell vaccines induce active immune surveillance against tumor cells in the brain by the dendritic cell-mediated presentation of antigens to T cells of the adaptive immune system.

https://doi.org/10.3348/kjr.2020.1450

Korean Journal of Radiology
KJR

With oncolytic viral therapy, viruses that selectively infect or replicate in tumor cells are created, resulting in the destruction of the infected tumor cells and the activation of pathways of immunogenic tumor cell death.

Genetically modified CAR T cells are another promising immunotherapy approach. T cells extracted from a patient's blood are genetically modified to recognize tumor-associated antigens and to signal T cells to kill tumor cells [58].

Approximately 2–14% of patients treated with immune-checkpoint inhibitors have been shown to develop new or enlarged enhancing lesions (which might mimic tumor progression) and a subsequent decrease in tumor burden, also known as pseudoprogression (Fig. 12). Early imaging findings that appear worse following immunotherapy might be associated with an inflammatory response directed against infiltrative brain tumor cells. Therefore, the immunotherapy Response Assessment for Neuro-Oncology (iRANO) criteria recommends that tumor response to immunotherapy be assessed and that radiographic progression be confirmed on follow-up imaging when progressive change is seen within 6 months of initiating immunotherapy [59].

Convection-Enhanced Delivery Therapy (Figure 13)

Convection-enhanced delivery therapy is a promising technique that generates a pressure gradient at the tip of an infusion catheter to deliver therapies directly into a brain tumor [60], resulting in high local concentrations of the drug with minimal systemic absorption. An implantable catheter system enables repeated administration of drugs to the brain through a port mounted on the skull [61]. In addition, drug distribution can be monitored in vivo by infusion of surrogate tracers such as gadolinium along with therapeutics [62]. High signal intensity from administered gadolinium during treatment should not be misinterpreted as an enhancing tumor on follow-up imaging.

Laser Interstitial Thermal Therapy (Figure 14)

Laser interstitial thermal therapy (LITT), a stereotactically guided percutaneous procedure, delivers light energy to target tissue via a fiberoptic catheter, resulting in selective thermal ablation of the lesions [63]. MRIs may be helpful for monitoring tissue ablation in real time during the procedure and for evaluating the effectiveness of ablation after therapy. Radiologists should be aware of the normal temporal radiographic evolution of the treated lesions. Within 24 hours, ablated lesions demonstrate a thin peripheral rim of enhancement and tend to enlarge during the first 40 days, followed by a continuous reduction in size thereafter [64]. Residual enhancement may persist during

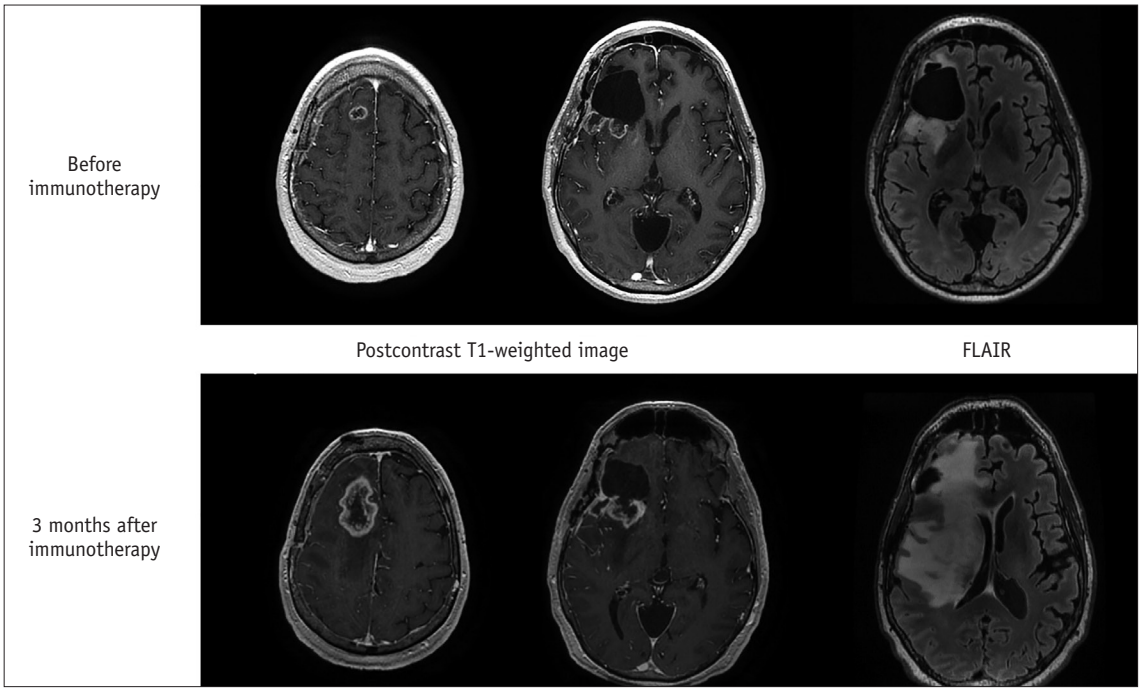

Fig. 12. A 64-year-old male with recurrent glioblastoma shows heterogeneous enhancing masses with perilesional edema at the posterior resection margin and in the right superior frontal gyrus. MRIs obtained 3 months after immunotherapy demonstrate marked enlargement of enhancing lesions with progression of edema, suggesting pseudoprogression. FLAIR = fluid-attenuated inversion-recovery

https://doi.org/10.3348/kjr.2020.1450

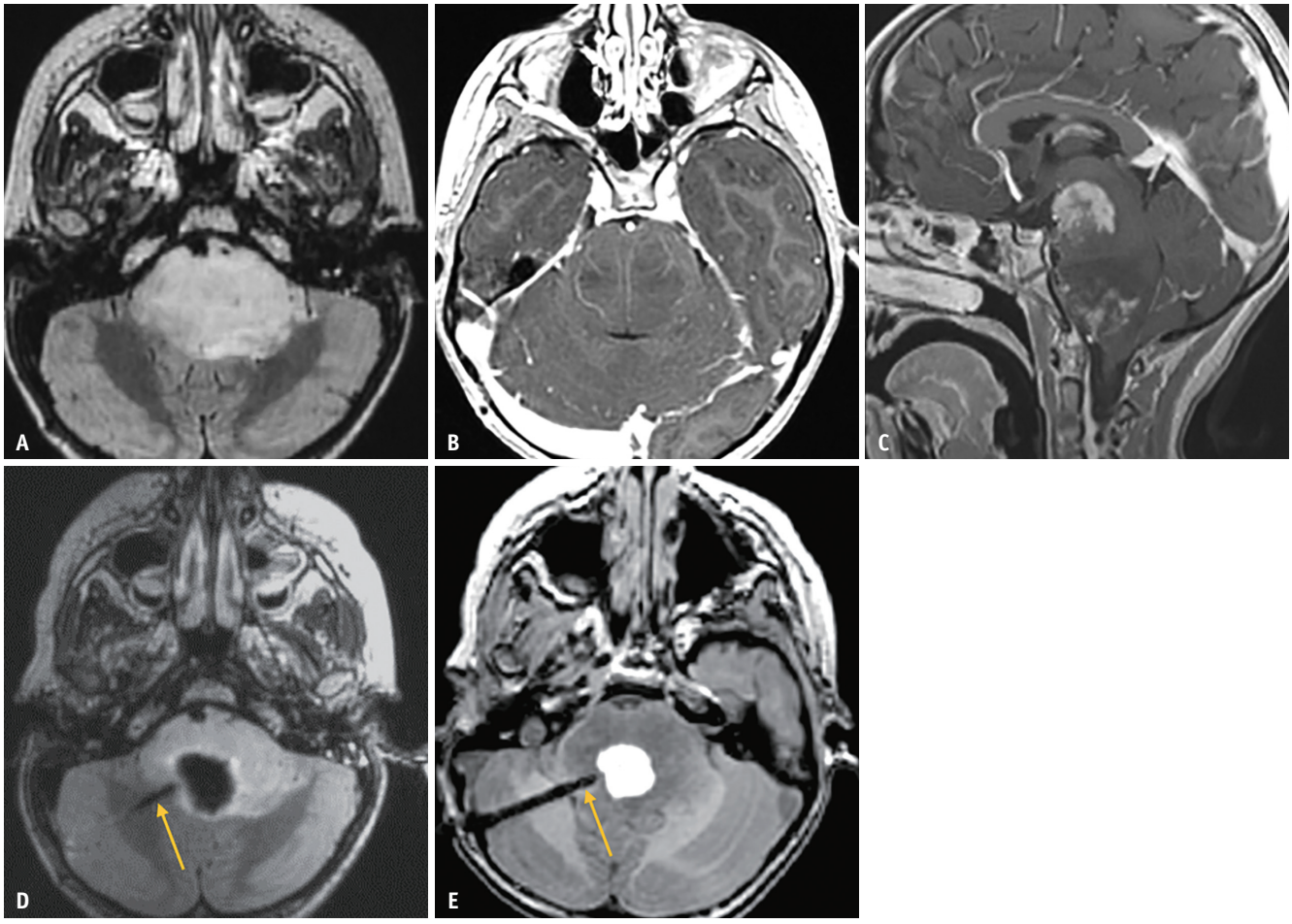

Fig. 13. A 7-year-old girl with diffuse intrinsic pontine glioma.
A-E. Expansile T2 hyperintense mass with heterogeneous enhancement predominantly involving the pons on FLAIR **(A)** and on axial and sagittal postcontrast T1WI **(B, C)**. MRIs obtained during convection-enhanced delivery demonstrate an infusion catheter (arrows) and drug delivery showing low signal intensity on FLAIR **(D)** and high signal intensity on T1WI **(E)** as gadolinium was administered along with therapeutics. FLAIR = fluid-attenuated inversion-recovery, T1WI = T1-weighted image

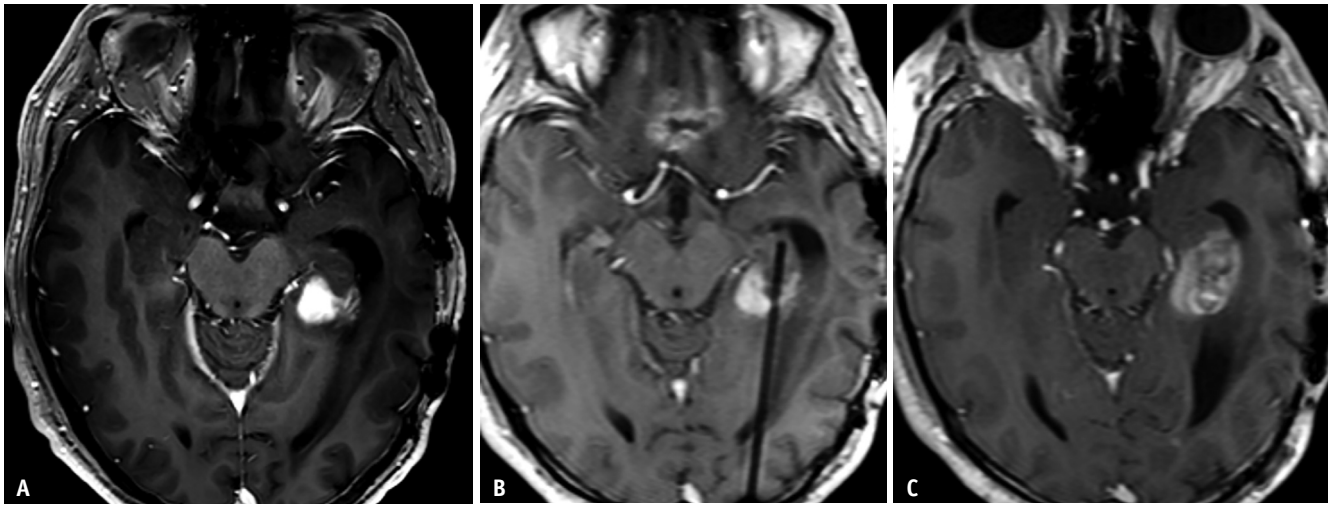

Fig. 14. A 38-year-old male with glioblastoma.
A-C. Before LITT **(A)**, homogeneously enhancing tumor is seen in the left mesial temporal lobe on postcontrast T1-weighted image. During LITT **(B)**, fiberoptic catheter targeting the tumor is seen on MRI. Four weeks after LITT **(C)**, the lesion shows interval enlargement of the enhancing tumor. LITT = laser interstitial thermal therapy

https://doi.org/10.3348/kjr.2020.1450

Korean Journal of Radiology
KJR

long-term follow-up, likely due to reactive inflammation or granulation tissue.

SUMMARY

In summary, the current trend toward the molecular characterization of CNS tumors will continue to advance. The use of imaging biomarkers for noninvasive profiling of specific molecular tumors will also advance and become part of the integrated diagnosis and be used to guide treatment planning for clinical studies and to optimize patient care. To maximally contribute to patient care, radiologists must be aware of the current tumor classification system and recognize specific imaging features following various treatments that allow for an accurate assessment of the response.

Conflicts of Interest

The authors have no potential conflicts of interest to disclose.

Author Contributions

Conceptualization: all authors. Supervision: Soonmee Cha. Writing—original draft: Sung Soo Ahn. Writing—review & editing: Soonmee Cha.

ORCID iDs

Sung Soo Ahn
https://orcid.org/0000-0002-0503-5558
Soonmee Cha
https://orcid.org/0000-0002-5924-5876

REFERENCES

1. Louis DN, Perry A, Reifenberger G, von Deimling A, Figarella-Branger D, Cavenee WK, et al. The 2016 World Health Organization classification of tumors of the central nervous system: a summary. *Acta Neuropathol* 2016;131:803-820
2. Hu LS, Ning S, Eschbacher JM, Baxter LC, Gaw N, Ranjbar S, et al. Radiogenomics to characterize regional genetic heterogeneity in glioblastoma. *Neuro Oncol* 2017;19:128-137
3. Park YW, Han K, Ahn SS, Bae S, Choi YS, Chang JH, et al. Prediction of IDH1-mutation and 1p/19q-codeletion status using preoperative MR imaging phenotypes in lower grade gliomas. *AJNR Am J Neuroradiol* 2018;39:37-42
4. Kratochwil C, Combs SE, Leotta K, Afshar-Oromieh A, Rieken S, Debus J, et al. Intra-individual comparison of ^{18}F-FET and ^{18}F-DOPA in PET imaging of recurrent brain tumors. *Neuro Oncol* 2014;16:434-440
5. Herrmann K, Czernin J, Cloughesy T, Lai A, Pomykala KL, Benz MR, et al. Comparison of visual and semiquantitative analysis of 18F-FDOPA-PET/CT for recurrence detection in glioblastoma patients. *Neuro Oncol* 2014;16:603-609
6. Kim HS, Goh MJ, Kim N, Choi CG, Kim SJ, Kim JH. Which combination of MR imaging modalities is best for predicting recurrent glioblastoma? Study of diagnostic accuracy and reproducibility. *Radiology* 2014;273:831-843
7. Kong DS, Kim ST, Kim EH, Lim DH, Kim WS, Suh YL, et al. Diagnostic dilemma of pseudoprogression in the treatment of newly diagnosed glioblastomas: the role of assessing relative cerebral blood flow volume and oxygen-6-methylguanine-DNA methyltransferase promoter methylation status. *AJNR Am J Neuroradiol* 2011;32:382-387
8. Louis DN, Ellison DW, Brat DJ, Aldape K, Capper D, Hawkins C, et al. cIMPACT-NOW: a practical summary of diagnostic points from Round 1 updates. *Brain Pathol* 2019;29:469-472
9. Batchala PP, Muttikkal TJE, Donahue JH, Patrie JT, Schiff D, Fadul CE, et al. Neuroimaging-based classification algorithm for predicting 1p/19q-codeletion status in IDH-mutant lower grade gliomas. *AJNR Am J Neuroradiol* 2019;40:426-432
10. Lee MK, Park JE, Jo Y, Park SY, Kim SJ, Kim HS. Advanced imaging parameters improve the prediction of diffuse lower-grade gliomas subtype, IDH mutant with no 1p19q codeletion: added value to the T2/FLAIR mismatch sign. *Eur Radiol* 2020;30:844-854
11. Patel SH, Poisson LM, Brat DJ, Zhou Y, Cooper L, Snuderl M, et al. T2–FLAIR mismatch, an imaging biomarker for IDH and 1p/19q status in lower-grade gliomas: a TCGA/TCIA project. *Clin Cancer Res* 2017;23:6078-6085
12. Cancer Genome Atlas Research Network, Brat DJ, Verhaak RG, Aldape KD, Yung WK, Salama SR, et al. Comprehensive, integrative genomic analysis of diffuse lower-grade gliomas. *N Engl J Med* 2015;372:2481-2498
13. Suh CH, Kim HS, Jung SC, Choi CG, Kim SJ. Imaging prediction of isocitrate dehydrogenase (IDH) mutation in patients with glioma: a systemic review and meta-analysis. *Eur Radiol* 2019;29:745-758
14. Park YW, Han K, Ahn SS, Choi YS, Chang JH, Kim SH, et al. Whole-tumor histogram and texture analyses of DTI for evaluation of IDH1-mutation and 1p/19q-codeletion status in World Health Organization Grade II gliomas. *AJNR Am J Neuroradiol* 2018;39:693-698
15. Zhou H, Vallières M, Bai HX, Su C, Tang H, Oldridge D, et al. MRI features predict survival and molecular markers in diffuse lower-grade gliomas. *Neuro Oncol* 2017;19:862-870
16. Chang K, Bai HX, Zhou H, Su C, Bi WL, Agbodza E, et al. Residual convolutional neural network for the determination of IDH status in low-and high-grade gliomas from MR imaging. *Clin Cancer Res* 2018;24:1073-1081
17. Choi C, Ganji SK, DeBerardinis RJ, Hatanpaa KJ, Rakheja D, Kovacs Z, et al. 2-hydroxyglutarate detection by magnetic resonance spectroscopy in IDH-mutated patients with gliomas. *Nat Med* 2012;18:624-629

 https://doi.org/10.3348/kjr.2020.1450

18. Verger A, Stoffels G, Bauer EK, Lohmann P, Blau T, Fink GR, et al. Static and dynamic ^{18}F-FET PET for the characterization of gliomas defined by IDH and 1p/19q status. *Eur J Nucl Med Mol Imaging* 2018;45:443-451
19. Lohmann P, Lerche C, Bauer EK, Steger J, Stoffels G, Blau T, et al. Predicting IDH genotype in gliomas using FET PET radiomics. *Sci Rep* 2018;8:13328
20. Park YW, Ahn SS, Park CJ, Han K, Kim EH, Kang SG, et al. Diffusion and perfusion MRI may predict EGFR amplification and the TERT promoter mutation status of IDH-wildtype lower-grade gliomas. *Eur Radiol* 2020;30:6475-6484
21. Stupp R, Mason WP, van den Bent MJ, Weller M, Fisher B, Taphoorn MJ, et al. Radiotherapy plus concomitant and adjuvant temozolomide for glioblastoma. *N Engl J Med* 2005;352:987-996
22. Lee S, Choi SH, Ryoo I, Yoon TJ, Kim TM, Lee SH, et al. Evaluation of the microenvironmental heterogeneity in high-grade gliomas with IDH1/2 gene mutation using histogram analysis of diffusion-weighted imaging and dynamic-susceptibility contrast perfusion imaging. *J Neurooncol* 2015;121:141-150
23. Price SJ, Allinson K, Liu H, Boonzaier NR, Yan JL, Lupson VC, et al. Less invasive phenotype found in isocitrate dehydrogenase–mutated glioblastomas than in isocitrate dehydrogenase wild-type glioblastomas: a diffusion-tensor imaging study. *Radiology* 2017;283:215-221
24. Hegi ME, Diserens AC, Gorlia T, Hamou MF, de Tribolet N, Weller M, et al. MGMT gene silencing and benefit from temozolomide in glioblastoma. *N Engl J Med* 2005;352:997-1003
25. Suh CH, Kim HS, Jung SC, Choi CG, Kim SJ. Clinically relevant imaging features for MGMT promoter methylation in multiple glioblastoma studies: a systematic review and meta-analysis. *AJNR Am J Neuroradiol* 2018;39:1439-1445
26. Solomon DA, Wood MD, Tihan T, Bollen AW, Gupta N, Phillips JJ, et al. Diffuse midline gliomas with histone H3-K27M mutation: a series of 47 cases assessing the spectrum of morphologic variation and associated genetic alterations. *Brain Pathol* 2016;26:569-580
27. Aboian MS, Solomon DA, Felton E, Mabray MC, Villanueva-Meyer JE, Mueller S, et al. Imaging characteristics of pediatric diffuse midline gliomas with histone H3 K27M mutation. *AJNR Am J Neuroradiol* 2017;38:795-800
28. Jung JS, Choi YS, Ahn SS, Yi S, Kim SH, Lee SK. Differentiation between spinal cord diffuse midline glioma with histone H3 K27M mutation and wild type: comparative magnetic resonance imaging. *Neuroradiology* 2019;61:313-322
29. Koeller KK, Rushing EJ. From the archives of the AFIP: pilocytic astrocytoma: radiologic-pathologic correlation. *Radiographics* 2004;24:1693-1708
30. Alkonyi B, Nowak J, Gnekow AK, Pietsch T, Warmuth-Metz M. Differential imaging characteristics and dissemination potential of pilomyxoid astrocytomas versus pilocytic astrocytomas. *Neuroradiology* 2015;57:625-638
31. Holderfield M, Deuker MM, McCormick F, McMahon M. Targeting RAF kinases for cancer therapy: BRAF-mutated melanoma and beyond. *Nat Rev Cancer* 2014;14:455-467
32. Schindler G, Capper D, Meyer J, Janzarik W, Omran H, Herold-Mende C, et al. Analysis of BRAF V600E mutation in 1,320 nervous system tumors reveals high mutation frequencies in pleomorphic xanthoastrocytoma, ganglioglioma and extra-cerebellar pilocytic astrocytoma. *Acta Neuropathol* 2011;121:397-405
33. Koeller KK, Henry JM. From the archives of the AFIP: superficial gliomas: radiologic-pathologic correlation. Armed Forces Institute of Pathology. *Radiographics* 2001;21:1533-1556
34. Hsu C, Kwan G, Lau Q, Bhuta S. Rosette-forming glioneuronal tumour: imaging features, histopathological correlation and a comprehensive review of literature. *Br J Neurosurg* 2012;26:668-673
35. Mack SC, Taylor MD. Put away your microscopes: the ependymoma molecular era has begun. *Curr Opin Oncol* 2017;29:443-447
36. Parker M, Mohankumar KM, Punchihewa C, Weinlich R, Dalton JD, Li Y, et al. C11orf95-RELA fusions drive oncogenic NF-κB signalling in ependymoma. *Nature* 2014;506:451-455
37. Nowak J, Jünger ST, Huflage H, Seidel C, Hohm A, Vandergrift LA, et al. MRI phenotype of RELA-fused pediatric supratentorial ependymoma. *Clin Neuroradiol* 2019;29:595-604
38. Cavalli FMG, Remke M, Rampasek L, Peacock J, Shih DJH, Luu B, et al. Intertumoral heterogeneity within medulloblastoma subgroups. *Cancer Cell* 2017;31:737-754.e6
39. Perreault S, Ramaswamy V, Achrol AS, Chao K, Liu TT, Shih D, et al. MRI surrogates for molecular subgroups of medulloblastoma. *AJNR Am J Neuroradiol* 2014;35:1263-1269
40. Iv M, Zhou M, Shpanskaya K, Perreault S, Wang Z, Tranvinh E, et al. MR imaging–based radiomic signatures of distinct molecular subgroups of medulloblastoma. *AJNR Am J Neuroradiol* 2019;40:154-161
41. Raybaud C, Ramaswamy V, Taylor MD, Laughlin S. Posterior fossa tumors in children: developmental anatomy and diagnostic imaging. *Childs Nerv Syst* 2015;31:1661-1676
42. AlRayahi J, Zapotocky M, Ramaswamy V, Hanagandi P, Branson H, Mubarak W, et al. Pediatric brain tumor genetics: what radiologists need to know. *Radiographics* 2018;38:2102-2122
43. Dangouloff-Ros V, Tauziède-Espariat A, Roux CJ, Levy R, Grévent D, Brunelle F, et al. CT and multimodal MR imaging features of embryonal tumors with multilayered rosettes in children. *AJNR Am J Neuroradiol* 2019;40:732-736
44. Shih RY, Koeller KK. Embryonal tumors of the central nervous system: from the radiologic pathology archives. *Radiographics* 2018;38:525-541
45. Weon YC, Kim EY, Kim HJ, Byun HS, Park K, Kim JH. Intracranial solitary fibrous tumors: imaging findings in 6 consecutive

https://doi.org/10.3348/kjr.2020.1450

patients. *AJNR Am J Neuroradiol* 2007;28:1466-1469
46. Smith JS, Cha S, Mayo MC, McDermott MW, Parsa AT, Chang SM, et al. Serial diffusion-weighted magnetic resonance imaging in cases of glioma: distinguishing tumor recurrence from postresection injury. *J Neurosurg* 2005;103:428-438
47. Wen PY, Macdonald DR, Reardon DA, Cloughesy TF, Sorensen AG, Galanis E, et al. Updated response assessment criteria for high-grade gliomas: response assessment in neuro-oncology working group. *J Clin Oncol* 2010;28:1963-1972
48. Yun TJ, Park CK, Kim TM, Lee SH, Kim JH, Sohn CH, et al. Glioblastoma treated with concurrent radiation therapy and temozolomide chemotherapy: differentiation of true progression from pseudoprogression with quantitative dynamic contrast-enhanced MR imaging. *Radiology* 2015;274:830-840
49. Vrabec M, Van Cauter S, Himmelreich U, Van Gool SW, Sunaert S, De Vleeschouwer S, et al. MR perfusion and diffusion imaging in the follow-up of recurrent glioblastoma treated with dendritic cell immunotherapy: a pilot study. *Neuroradiology* 2011;53:721-731
50. Kim JY, Park JE, Jo Y, Shim WH, Nam SJ, Kim JH, et al. Incorporating diffusion- and perfusion-weighted MRI into a radiomics model improves diagnostic performance for pseudoprogression in glioblastoma patients. *Neuro Oncol* 2019;21:404-414
51. Park YW, Ahn SS, Kim EH, Kang SG, Chang JH, Kim SH, et al. Differentiation of recurrent diffuse glioma from treatment-induced change using amide proton transfer imaging: incremental value to diffusion and perfusion parameters. *Neuroradiology* 2021;63:363-372
52. van Dijken BRJ, van Laar PJ, Holtman GA, van der Hoorn A. Diagnostic accuracy of magnetic resonance imaging techniques for treatment response evaluation in patients with high-grade glioma, a systematic review and meta-analysis. *Eur Radiol* 2017;27:4129-4144
53. Galldiks N, Lohmann P, Albert NL, Tonn JC, Langen KJ. Current status of PET imaging in neuro-oncology. *Neurooncol Adv* 2019;1:vdz010
54. Nihashi T, Dahabreh IJ, Terasawa T. Diagnostic accuracy of PET for recurrent glioma diagnosis: a meta-analysis. *AJNR Am J Neuroradiol* 2013;34:944-950, S1-S11
55. Rieger J, Bähr O, Müller K, Franz K, Steinbach J, Hattingen E. Bevacizumab-induced diffusion-restricted lesions in malignant glioma patients. *J Neurooncol* 2010;99:49-56
56. Nguyen HS, Milbach N, Hurrell SL, Cochran E, Connelly J, Bovi JA, et al. Progressing bevacizumab-induced diffusion restriction is associated with coagulative necrosis surrounded by viable tumor and decreased overall survival in patients with recurrent glioblastoma. *AJNR Am J Neuroradiol* 2016;37:2201-2208
57. Lim M, Xia Y, Bettegowda C, Weller M. Current state of immunotherapy for glioblastoma. *Nat Rev Clin Oncol* 2018;15:422-442
58. Brown CE, Alizadeh D, Starr R, Weng L, Wagner JR, Naranjo A, et al. Regression of glioblastoma after chimeric antigen receptor T-cell therapy. *N Engl J Med* 2016;375:2561-2569
59. Okada H, Weller M, Huang R, Finocchiaro G, Gilbert MR, Wick W, et al. Immunotherapy response assessment in neuro-oncology: a report of the RANO working group. *Lancet Oncol* 2015;16:e534-e542
60. Mehta AM, Sonabend AM, Bruce JN. Convection-enhanced delivery. *Neurotherapeutics* 2017;14:358-371
61. Sonabend AM, Stuart RM, Yun J, Yanagihara T, Mohajed H, Dashnaw S, et al. Prolonged intracerebral convection-enhanced delivery of topotecan with a subcutaneously implantable infusion pump. *Neuro Oncol* 2011;13:886-893
62. Mardor Y, Rahav O, Zauberman Y, Lidar Z, Ocherashvilli A, Daniels D, et al. Convection-enhanced drug delivery: increased efficacy and magnetic resonance image monitoring. *Cancer Res* 2005;65:6858-6863
63. Medvid R, Ruiz A, Komotar RJ, Jagid JR, Ivan ME, Quencer RM, et al. Current applications of MRI-guided laser interstitial thermal therapy in the treatment of brain neoplasms and epilepsy: a radiologic and neurosurgical overview. *AJNR Am J Neuroradiol* 2015;36:1998-2006
64. Schwabe B, Kahn T, Harth T, Ulrich F, Schwarzmaier HJ. Laser-induced thermal lesions in the human brain: short- and long-term appearance on MRI. *J Comput Assist Tomogr* 1997;21:818-825

 https://doi.org/10.3348/kjr.2020.1450